MULTIVARIABLE CLOSED-LOOP CONTROL OF THE REATTACHMENT LENGTH DOWNSTREAM OF A BACKWARD-FACING STEP

Lars Henning and Rudibert King [1]

Measurement and Control Group
Institute of Process and Plant Technology
Berlin University of Technology
Hardenbergstraße 36a, 10623 Berlin, Germany

Abstract: Active control of separated flows has become a major challenge in recent years. Whereas most of the work published so far is based on simulation studies this paper gives an example of a successful application of a multivariable closed-loop flow control in wind tunnel experiments. A robust $\mathcal{H}_\infty$-controller is used to control the spanwise reattachment length downstream of a benchmark problem, a so-called backward-facing step. The synthesis of the controller is based on a family of identified linear black-box models. To reduce the conservatism of this approach, a nonlinear static precompensation is included. Tracking performance and disturbance rejection of the controller are tested in wind tunnel experiments.

Keywords: backward-facing step, black-box model, flow control, $\mathcal{H}_\infty$-controller, multivariable control, reattachment length

1. INTRODUCTION

Flow separations on swept airfoils of varying chord length, in turbo-machines or behind bluff bodies, such as automobiles, show complex space- and time-dependent profiles. Flow separation accounts for negative effects such as a reduced lift and an increased drag of an airfoil, noise production and efficiency-loss in turbines or increasing aerodynamic drag behind trucks or ships. In combustion cambers, however, a recirculation region as a result of flow separation is desired to keep the fuel mixture in the reaction zone for a complete combustion.

Thus, the suppression or a desired control of separation phenomena has been addressed in the fluid dynamics community for many decades. For a long time, only passive means have been considered. However, when shaping of the geometry has reached an optimum or when passive means, such as vortex generator, have positive and negative effects, active devices in open- or closed-loop control can further improve the performance by suction and blowing, acoustic actuation or magneto-hydrodynamic forces. Furthermore, active flow control is able to adapt the actuation to a wide range of operating conditions in an optimal sense. The first real active flow control demonstration for an airplane was done 2003 with a XV-15 tilt-rotor aircraft (Wygnanski, 2004).

Most of the work published so far is dedicated to open-loop control. Literature surveys on feed-

[1] Corresponding author, email: rudibert.king@tu-berlin.de, web: http://mrt.tu-berlin.de

forward flow control, including actuation mechanisms and sensor applications, are given in (Fiedler and Fernholz, 1990), or (Gad-el-Hak *et al.*, 1998).

In contrast, the present investigation focusses on the closed-loop control of separated flows by active means to profit from the well-known advantages such as disturbance rejection and set-point tracking. It differs from the majority of the so far published work in this field with respect to two important features: I) The developed closed-loop controller is applied in a real experiment. II) It is shown that variable spatial profiles can be controlled as well to address problems such as separation control on swept airfoils with non-constant chord length in the future.

Different approaches to synthesize controllers based on the solution of the Navier Stokes equations or based on physically derived nonlinear low-dimensional models are surveyed in (Becker *et al.*, 2004) together with black-box-type approaches.

Experimental validations of closed-loop flow control are still rare. In (Allan *et al.*, 2000) tuning rules are used for the control of a generic model of an airfoil. (Glauser *et al.*, 2004) uses the first mode of a proper orthogonal decomposition of an airfoil with a proportional controller. In (Becker *et al.*, 2004) robust SISO-controllers are synthesised based on identified models for the backward-facing step. A comparison of this SISO-controller with a flatness based controller is given in (Becker and King, 2005) and adaptive MISO-controllers are used in (Garwon and King, 2005). More successful applications of closed-loop flow control in wind tunnel experiments are given in (King *et al.*, 2004) as well for other flow configurations. A black-box approach is chosen as well in experimental burner control studies. Pressure fluctuations in combustion chambers are controlled in (Annaswamy *et al.*, 2000) and Tollmien-Schlichting-waves are rejected using a FIR-based controller in (Baumann and Nitsche, 1996) for an airfoil.

The paper is organised as follows: The flow configuration is given in section 2 with an emphasis on the physical processes exploited by the control and the sensor concept used. Section 3 and section 4 describe the controller synthesis and experimental results, respectively.

2. FLOW CONFIGURATION

2.1 General description

The backward-facing step flow has been established as a benchmark problem for separated flows in fluid dynamics, first. A variety of information about the flow process and actuation mechanisms is available, see for example (Wengle *et al.*, 2001) or (Jürgens and Kaltenbach, 2003) for a swept backward-facing step. A sketch of the flow field for a 2D-actuation is given in Fig. 1, where the oncoming flow with the free-stream velocity U_∞ detaches at the edge of the step and reattaches downstream. Four different regimes exist in the wake: a recirculation zone, also called separation bubble, the shear layer above the recirculation zone, a reattachment zone, and a newly developing boundary layer downstream of the reattachment zone.

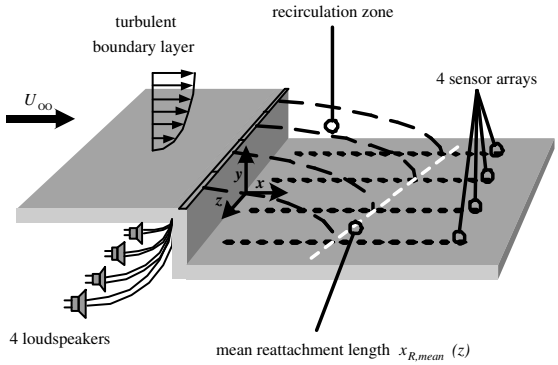

Fig. 1. Configuration of the backward-facing step with four loudspeakers and four sensor arrays for actuation and sensing as a function of the spanwise coordinate.

The shear layer is governed by the Kelvin-Helmholz instability phenomenon. Perturbations are amplified leading to vortex shedding with the natural frequency f_{shear}. Hence, for uniform actuation with all loudspeakers the shear layer rolls up into two-dimensional, coherent vortical structures called vortices in the following. These vortices convect downstream with approximately the half free-stream velocity. In the MIMO-case three-dimensional structures are formed.

The recirculation bubble is characterized by pressure driven inflow and outflow caused by shear layer entrainment. While negative skin-friction, i.e. reverse flow, occurs in the recirculation zone, the reattachment position is characterized by zero friction. Downstream a new boundary layer develops causing positive skin-friction, i.e. forward flow.

The vortex generated entrainment mechanism in the shear layer is enhanced by the acoustic actuation of the detaching boundary layer at the edge of the step, as shown in Fig. 1. Slot-loudspeaker actuators are used for this. As the Kelvin-Helmholz instability phenomenon is triggered by the input, only a small amount of energy is needed which leads to an unstable growth of actuated perturbations. Therefore, the actuation frequency should

be near the natural instability frequency, $f_\mathrm{a} \approx f_\mathrm{shear}$. The amplitude of the harmonic loudspeaker signal finally affects the initial size of the growing vortices and, thus, the reattachment length. Hence, the amplitude is the input for the control problem.

Since the reattachment length characterizes the size of the separation bubble it is taken as the primary variable to be controlled. In this benchmark configuration, the goal is to control the reattachment length as a function of the spanwise coordinate z using distributed actuation. Therefore, the reattachment length is referred to $x_\mathrm{R}(z,t)$ in the following. A spanwise variable separation bubble might be of interest for flight control. By implying different spanwise profiles for the length of the separated regions above the airfoils on both sides of an airplane, roll moments could be imposed. Due to the very fast dynamics of loudspeakers or, alternatively, valves used to modulate a blowing air stream, a much faster response can be obtained compared to rather slow classical mechanical devices, such as flaps.

2.2 Experimental set-up

The experiments are conducted in an open-type wind tunnel. The test section is 1600×88×400 mm in the streamwise (x), transverse (y) and spanwise (z) directions, respectively. The step is located 27 step heights downstream of the test section inlet and the step height is $H = 20\,\mathrm{mm}$. All presented experiments are carried out with a step height based Reynolds number $Re_\mathrm{H} = U_\infty H/\nu = 25000$. The coordinate system is centred at the edge of the step.

For the spanwise distributed actuation the actuator slot is partitioned in the spanwise direction into four sections of equal length. Each slot is connected with an individual controllable loudspeaker. Here harmonic actuations $a_\mathrm{i} = a_{0,\mathrm{i}} \sin(2\pi f_\mathrm{a}\ t)$, $\mathrm{i} = 1,\ldots,4$, with actuation amplitudes $\mathbf{a}_0$ and actuation frequency f_a are applied. The specified optimal value of the dimensionless frequency (Strouhal number) relating to the Kelvin-Helmholz instability is about $St_{\delta_2} = f_\mathrm{a}\delta_2/U_\infty = 0.02$ based on the momentum thickness $\delta_2 = 0.07\,H$ of the boundary layer. The values of the amplitudes $\mathbf{a}_0$ give the amplitudes of the velocity signal that are provided by the loudspeakers.

The controller is implemented on a rapid prototyping hardware (dSPACE controller board 1005 PPC) with a typical sampling rate of 5000 Hz.

2.3 Sensor concept

In contrast to many other process control applications, measuring the output signal cannot be done in a straightforward manner. Although a variety of methods exist in fluid dynamics with which a time-averaged reattachment length $x_\mathrm{R,mean}(z,t)$ can be determined, see (Fernholz *et al.*, 1996), most of them cannot be used in a closed-loop setting. Some reasons are insufficient time resolution, missing on-line capabilities, missing two-dimensional or even one-dimensional information, or simply costs.

As a practical alternative, microphones are used for pressure measurements downstream of the backward-facing step. This method is based on the observation of (Mabey, 1972) that the root-mean-square value (RMS-value) of the pressure fluctuations p'_rms downstream of the backward-facing step passes through a strongly marked maximum. For the experiments considered here, this maximum lies at approx. 86% of the time-averaged reattachment length $x_{R,mean}(z)$. This method is called RMS-method in the following. For the measurement of the pressure fluctuations 4×15 mirophones (Sennheiser, KE 4-211-2) in parallel rows downstream of the step are applied. These microphone rows are located at z/H = -6.9, -2.3, 2.3, 6.9, see Fig. 1.

Fig. 2 displays the RMS-values downstream the step in different spanwise positions for distributed actuation. The streamwise coordinate is normalized by the mean reattachment length $x_{R,mean}(z)$ which is obtained by standard oil-film interferometry. Although different actuation amplitudes are used for the four loudspeakers, the maxima of p'_rms are relatively constant with respect to $x_{R,mean}(z)$. From these measurements it can be concluded that by means of an on-line fit of a 5th-order polynomial to the measured RMS-values the maxima and thereby $x_\mathrm{R,mean}(z,t)$ can be estimated.

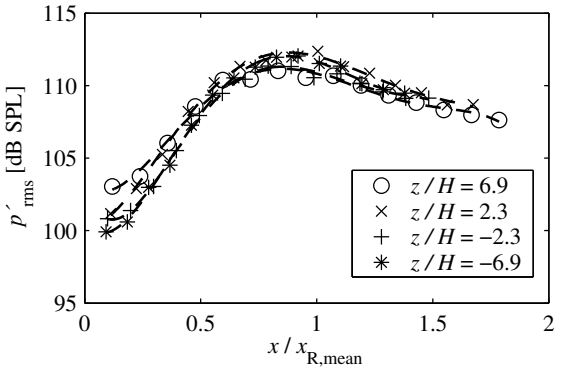

Fig. 2. Relative positions of RMS-values of the pressure fluctuations using distributed actuation. $Re_\mathrm{H} = 25000$, $St_{\delta_2} = 0.02$, $\mathbf{a}_0/U_\infty$ = (0.06, 0.02, 0.01, 0.0).

3. MODEL IDENTIFICATION AND CONTROLLER SYNTHESIS

To show the coupling effect of a spanwise distributed actuation, i.e. a true MIMO characteristic, the reduction of the reattachment length is given in Fig. 3 for two different situations. The size of the actuation amplitudes $\mathbf{a}_0$ of the four loudspeakers are given by the shaded bars. Especially in the left graph a coupling between the different channels is observed. Although the two inner speakers are switched off, a reduction of the recirculation length in the inner part behind the step is observed, too.

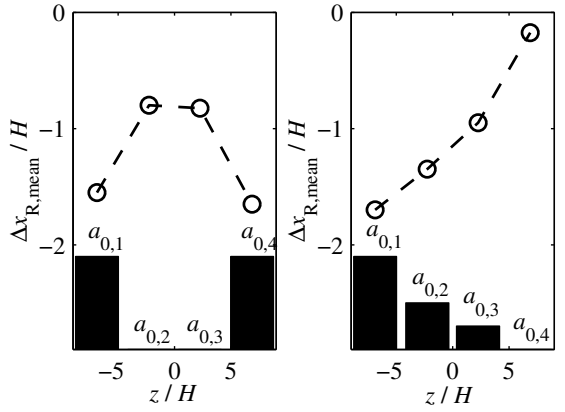

Fig. 3. Mean reduction of the reattachment length in spanwise direction for different actuation amplitudes $\mathbf{a}_0$. $Re_{\mathrm{H}} = 25000$, $St_{\delta_2} = 0.02$.

To identify linear black-box models step experiments are performed in which the actuation amplitudes $\mathbf{a}_0$ are switched from zero to different levels. A family of linear time-continuous multivariable models of 4th order with a time delay is identified by application of subspace methods. From these, a nominal model $\mathbf{G}_{\mathrm{N}}$ is generated which shows a minimum distance, here l_{M}, to all identified models over a certain frequency range. The plant $\mathbf{G}$ on which the robust controller synthesis is based, is then described by a multiplicative uncertainty $\mathbf{\Delta}_{\mathrm{M}}(j\omega)$:

$$\mathbf{G}(s) = \mathbf{G}_{\mathrm{N}}(s)(1 + \mathbf{\Delta}_{\mathrm{M}}(s)), \qquad (1)$$

$$\|\mathbf{\Delta}_{\mathrm{M}}(j\omega)\| \leq l_{\mathrm{M}}(\omega). \qquad (2)$$

The nonlinearity of the investigated backward-facing step flow causes a very wide spreading of the model parameters, i.e. a conservative controller design is required for robust closed-loop stability. Analysing the identified linear model family, a correlation between the amplitudes used for the step experiments and the values of the diagonal elements of the static gain matrix for different actuation amplitudes can be found. This

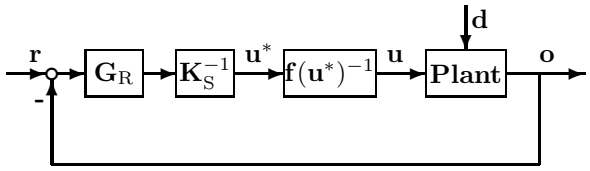

Fig. 4. Control-loop with two pre-compensators ($\mathbf{G}_{\mathrm{R}}$ - controller; **r** - reference; **u** - manipulated variable; **d** - disturbances; **o** - output).

dependency can be fitted by a static map $\mathbf{f}(\mathbf{u})$. With the inverse of this map the uncertainty of the models can be compensated, partially. Fig. 5 shows a comparison of singular values computed with compensated and non-compensated models.

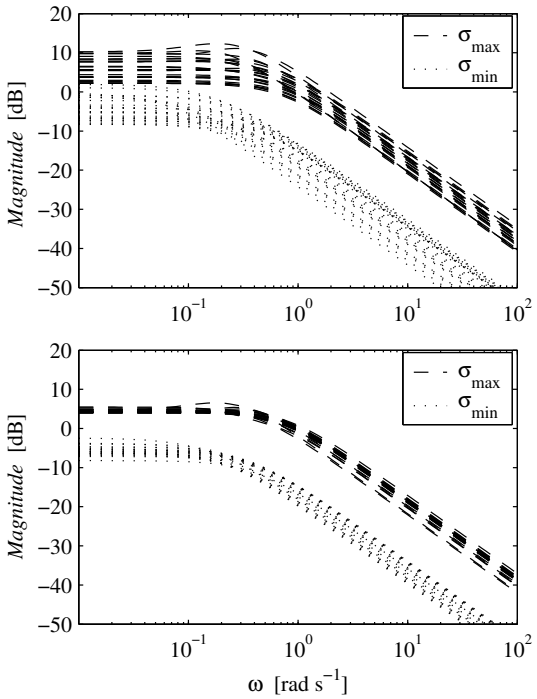

Fig. 5. Singular values of identified models. Non-compensated models (above) in comparison with compensated models (below).

The control loop is extended by a second pre-compensator for steady-state decoupling, which counteracts the interaction in the plant, see Fig. 4. This pre-compensator corresponds to the inverse of the static gain matrix of the nominal model $\mathbf{K}_{\mathrm{s}}^{-1}$.

For uncertain systems many mature controller synthesis methods do exist. Here, a $\mathcal{H}_\infty$-synthesis scheme is chosen. In $\mathcal{H}_\infty$-control stability and/or performance of the 'worst' plant used to describe the process can be guaranteed. For the controller synthesis the so-called mixed sensitivity problem is solved in which the controller is synthesized in such a way that a compromise between robust

stability, disturbance rejection and spent energy for control is met. This is done by using different frequency dependent weights with which different closed-loop specifications are combined. For more details the reader is referred to standard textbooks, e.g. (Skogestad and Postlethwaite, 1996).

4. EXPERIMENTAL RESULTS

The behaviour of the closed-loop control of the 4×4 MIMO-control system is tested in wind tunnel experiments with respect to tracking response and disturbance rejection.

Fig. 6 shows the tracking response of the closed-loop with the synthesized $\mathcal{H}_\infty$-controller at $Re_\mathrm{H} = 25000$. Shown is the reduction of the recirculation length above the four sensor arrays compared to the non-actuated case. A good tracking performance can observed. However, the controlled mean reattachment length follows the reference command with a delay due to the limited temporal resolution of the measurement of $x_{\mathrm{R,mean}}(z,t)$. Due to the averaging for the RMS-calculation, the temporal resolution of the RMS-method limits the achievable performance. Hence, rampwise changes of the reference command are applied, as with the RMS-method stepwise changes do not make sense.

A main advantage of closed-loop control in comparison to open-loop control is disturbance rejection. One possibility to massively disturb the backward-facing step flow is to reduce the cross-sectional area of the wind tunnel test section. Fig. 7 displays the behaviour of the mean reattachment length after placing a cuboid-shaped body ($7.5\,H \times 5\,H \times 2.5\,H$) in the wake of the backward-facing step at $x/H = 20$. This corresponds to a reduction of cross-sectional area of approx. 35%. The influence of the disturbance on the flow can be observed in the time series of the Reynolds number, shown in the upper part of Fig. 7. The reference command is set to a constant reduction of reattachement length $\Delta\mathbf{x}_\mathrm{R}/H = (-0.5, -1.0, -1.5, -2.0)$. In the time intervall $0 \leq t \leq 9\,\mathrm{s}$, the flow is not disturbanced, with $Re_\mathrm{H} = 25000$. The positioning of the body by hand in the time intervall $9 \leq t \leq 17\,\mathrm{s}$ leads to large fluctuations of the Reynolds number. A larger control error can be observed, initially. After the body is positioned ($t \geq 17\,\mathrm{s}$), however, the closed-loop control is able to compensate this disturbance fast.

5. CONCLUSION AND OUTLOOK

This example shows that robust control methods can be used for flow control problems in experiments. The proposed methodology utilises simple

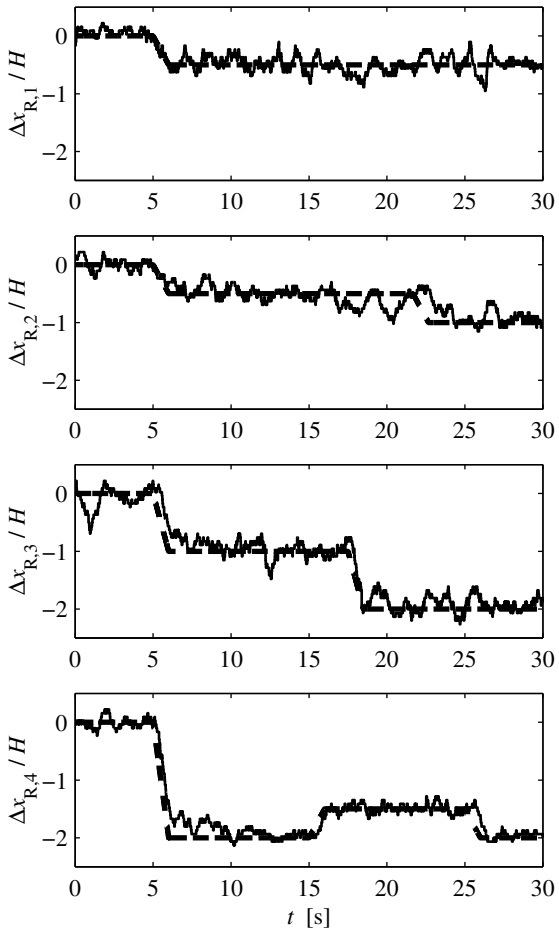

Fig. 6. Tracking response for 4×4 MIMO-control system at $Re_\mathrm{H} = 25000$. (−− reference command, – normalized reduction of the recirculation length)

black-box models with a static pre-compensation of the non-linear gain. The synthesized robust controller works for the control of the spanwise time-averaged reattachment length, as demonstrated in experiments.

The dynamics of the closed-loop control is affected by the used RMS-method. A better dynamic behaviour can expected by the application of sensor concepts with higher temporal and spatial resolution, such as micro-electro-mechanical systems (MEMS), miniature amplified low pressure sensors or model-based estimation schemes (Becker *et al.*, 2003).

In the future, the applied methods will be extended to more complex, three-dimensional flow configurations, e.g. a swept high-lift configuration, or a bluff body, such as the 'Ahmed body'.

6. ACHNOWLEDGMENTS

This work was founded by the German Science Foundation (DFG) as part of the Collaborative

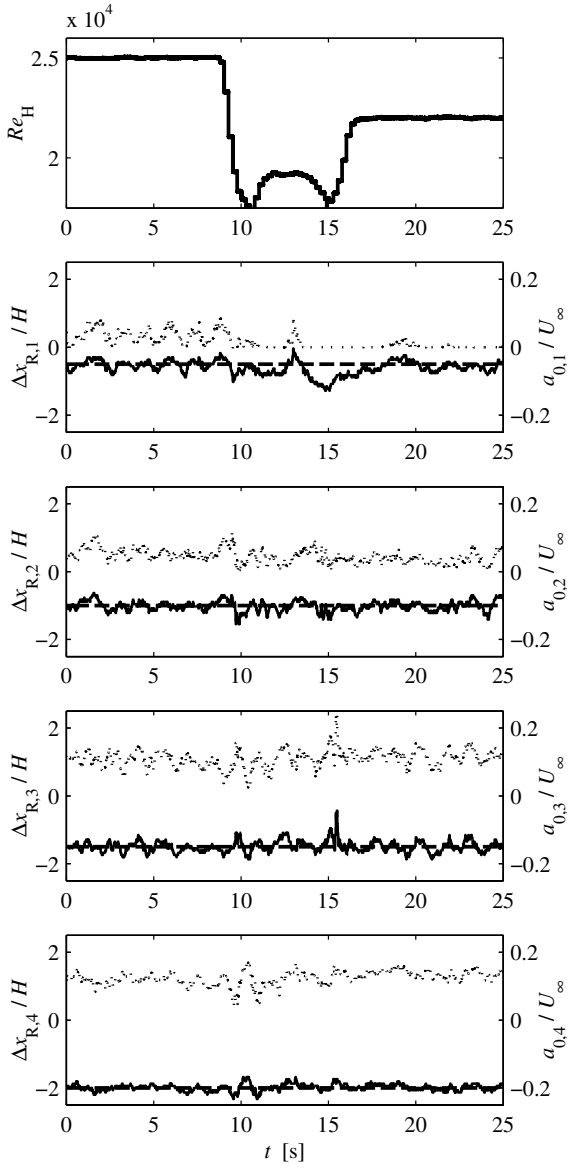

Fig. 7. Disturbance rejection of 4×4 MIMO-control system with massive disturbance by an approx. 35% reduction of the cross-sectional area of the wind tunnel test section, (−− reference command, – normalized reduction of the recirculation length, ··· normalizied actuation amplitude).

Research Centre (SFB 557) 'Control of complex turbulent shear flow'.

REFERENCES

Allan, B.G., J.-N. Juang, D.L. Raney, A. Seifert, L.G. Pack and D.E. Brown (2000). Closed loop separation control using oscillatory flow excitation. In: *ICASE Report 2000-32*.

Annaswamy, A., M. Fleifil, J. Rumsey, R. Prasanth, J. Hathout and A. Ghoniem (2000). Thermoacoustic instability: Model-based optimal control design and experimental validation. *IEEE Transactions on Control Systems Technology* **8**, 905–918.

Baumann, M. and W. Nitsche (1996). Investigation of active control of Tollmien-Schlichting waves on a wing. *Transitional boundary layers in Aeronautics* **46**, 89–98.

Becker, R. and R. King (2005). Comparison of a robust and a flatness based control for a separated shear flow. *Submitted to IFAC*.

Becker, R., M. Garwon and R. King (2003). Development of model-based sensors and their use for closed-loop control of separated shear flows. In: *Proc. of the ECC*. Cambridge.

Becker, R., M. Garwon, C. Gutknecht, G. Bärwolff and R. King (2004). Robust control of separated shear flows in simulation and experiment. *Submitted to J. Process Control*.

Fernholz, H.H., G. Janke, M. Schober, P.M. Wagner and D. Warnack (1996). New devolopments and applications of skin-friction measuring techniques. *Meas. Sci. Technol.* **7**, 1396–1409.

Fiedler, H.-E. and H.H. Fernholz (1990). On managment and control of turbulent shear flows. *Progr. Aeronaut. Sci.* **27**, 305–387.

Gad-el-Hak, M., A. Pollard and J.-P. Bonnet (1998). *Flow Control - Fundamentals and Practices*. Springer. Berlin, Heidelberg.

Garwon, M. and R. King (2005). A multivariable adaptive control strategy to regulate the separated flow behind a backward-facing step. *Submitted to IFAC*.

Glauser, M. N., H. Higuchi, J. Ausseur and J. Pinier (2004). Feedback control of separated flows. *AIAA-Paper 2004-2521*.

Jürgens, W. and H.-J. Kaltenbach (2003). Eigenmode decomposition of turbulent velocity fields behind a swept, backward-facing step. *J. of Turbulence*.

King, R., R. Becker, M. Garwon and L. Henning (2004). Robust and adaptive closed-loop control of separated shear flows. *AIAA-Paper 2004-2519*.

Mabey, D.G. (1972). Analysis and correlation of data on pressure fluctuations in separated flow. *J. Aircraft* **9**(9), 642–645.

Skogestad, S. and I. Postlethwaite (1996). *Multivariable Feedback Control - Analysis and Design*. John Wiley & Sons. Chichester, England.

Wengle, H., G. Bärwolff, G. Janke and A. Huppertz (2001). The manipulated transitional backward-facing step flow: an experimental and direct numerical simulation investigation. *Eur. J. Mech., B/Fluids* pp. 25–46.

Wygnanski, I. (2004). The variables affecting the control of separation by periodic excitation. *AIAA-Paper 2004-2505*.